

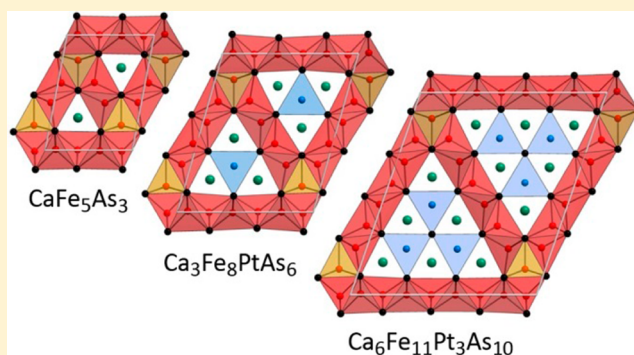
Framework Structures of Interconnected Layers in Calcium Iron Arsenides

Tobias Stürzer, Christine Hieke, Catrin Löhnert, Fabian Nitsche, Juliane Stahl, Christian Maak, Roman Pobel, and Dirk Johrendt*

Department Chemie, Ludwig-Maximilians-Universität München, Butenandtstrasse 5–13 (Haus D), 81377 München, Germany

Supporting Information

ABSTRACT: The new calcium iron arsenide compounds $\text{Ca}_{n(n+1)/2}(\text{Fe}_{1-x}\text{M}_x)_{(2+3n)}\text{M}'_{n(n-1)/2}\text{As}_{(n+1)(n+2)/2}$ ($n = 1–3$; $M = \text{Nb, Pd, Pt}$; $M' = \square, \text{Pd, Pt}$) were synthesized and their crystal structures determined by single-crystal X-ray diffraction. The series demonstrates the structural flexibility of iron arsenide materials, which otherwise prefer layered structures, as is known from the family of iron-based superconductors. In the new compounds, iron arsenide tetrahedral layers are bridged by iron-centered pyramids, giving rise to so far unknown frameworks of interconnected FeAs layers. Channels within the structures are occupied with calcium and palladium or platinum, respectively. Common basic building blocks are identified that lead to a better understanding of the building principles of these structures and their relation to CaFe_4As_3 .



INTRODUCTION

Layered iron arsenides have earned sweeping prominence in the solid-state chemistry and physics communities during the last years because of the emergence of high-temperature superconductivity up to 55 K.^{1–4} Therewith, the family of layered iron arsenides was found to be a new class of high- T_c superconductors beyond the copper oxides discovered in the 1980s.⁵ Intensive research has meanwhile identified a growing family of layered compounds each containing two-dimensional FeAs layers.⁶ A magnetic instability in the iron layers intertwined with the superconducting properties has been uncovered,⁷ which can be manipulated by chemical doping, pressure, or complete replacement of the separating layers by other two-dimensional structure fragments.^{6,8} The presence of layered structures in both high- T_c superconductor families has raised the question about the general necessity of low dimensionality, but no final consent has been found on this topic so far. Besides, other structures, featuring fragments of FeAs tetrahedral layers, are also expected to reveal very interesting properties, although it is not clear whether superconductivity could arise in such systems. In 2009, the compound CaFe_4As_3 with a structure consisting of interconnected $\text{FeAs}_{4/4}$ tetrahedral bands forming channels occupied with calcium was identified.⁹ At the band joints, iron is pyramidally coordinated by five arsenic ions connecting two bands. Magnetic measurements identified iron(II) in the $\text{FeAs}_{4/4}$ tetrahedra but also remarkably iron(I) in the $\text{FeAs}_{5/5}$ pyramids.¹⁰ Also, hints to a spin-density wave were reported similar to the layered compounds, but despite diverse substitution attempts, no superconducting properties were achieved.¹¹

In this paper, we report five new structure types in the iron arsenide family with the general composition $\text{Ca}_{n(n+1)/2}(\text{Fe}_{1-x}\text{M}_x)_{(2+3n)}\text{M}'_{n(n-1)/2}\text{As}_{(n+1)(n+2)/2}$ ($M = \text{Nb, Pd, Pt}$; $M' = \square, \text{Pd, Pt}$) with $n = 1–3$, featuring three-dimensional frameworks of interconnected layers. A structural breakdown of these compounds to basic building blocks is given, yielding a systematic understanding of the relationship of these structures to each other and their close relationship to CaFe_4As_3 as well as to layered iron pnictides. Finally, the connection to a long-known class of intermetallic compounds with a metal-to-pnictide ratio of 2:1 is illustrated.

EXPERIMENTAL SECTION

Polycrystalline samples of the compounds $\text{Ca}_{n(n+1)/2}(\text{Fe}_{1-x}\text{M}_x)_{(2+3n)}\text{M}'_{n(n-1)/2}\text{As}_{(n+1)(n+2)/2}$ with $n = 2$ and 3 and $(\text{Ca,Na})_3(\text{Fe,Nb})_8\text{As}_6$ were synthesized by solid-state methods under ambient pressure. Stoichiometric mixtures of pure elements (>99.5%) were heated at 900–1000 °C in alumina crucibles or niobium tubes, respectively, and sealed in silica tubes under purified argon. The samples were thoroughly homogenized and annealed twice at 900–1000 °C. The α -polymorphs of the compounds with $n = 1$ and 2 were synthesized from a mixture of binary starting materials and pure elements (>99.5%) by high-pressure synthesis in boron nitride crucibles at 6 GPa and 1000 °C, using a modified Walker-type multianvil apparatus.^{12,13}

Bulk α - $\text{Ca}_3\text{Fe}_8\text{PtAs}_6$ was obtained by both high-pressure and high-temperature synthesis, whereas CaFe_5As_3 was accessible only by high-pressure synthesis. β - $\text{Ca}_3\text{Fe}_8\text{PtAs}_6$ was only obtainable as a side phase. In the Ca–Fe–Pd–As system, solid-state synthesis always yielded a

Received: April 2, 2014

Published: June 2, 2014

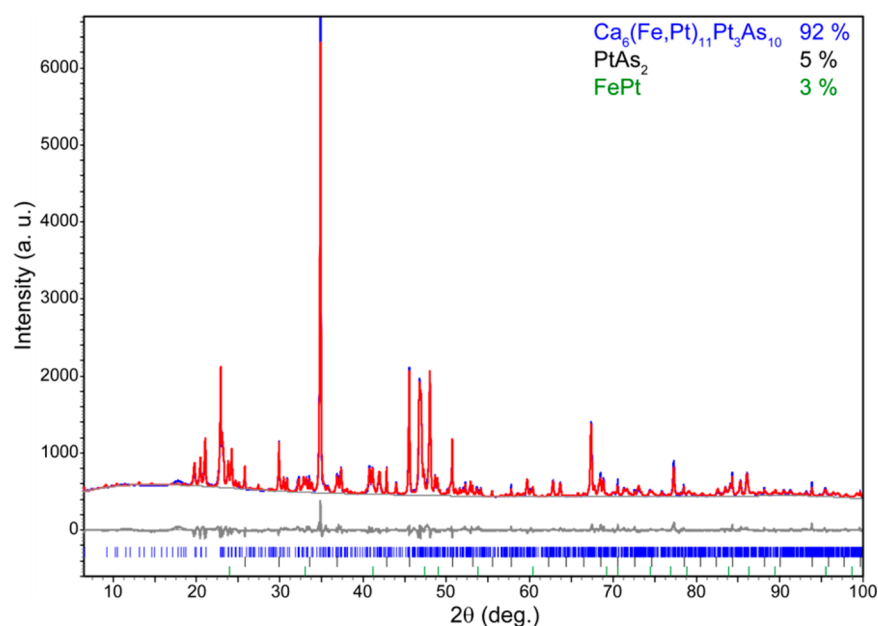


Figure 1. Powder X-ray diffraction pattern (blue) and Rietveld fit (red) of $\text{Ca}_6(\text{Fe,Pt})_{11}\text{Pt}_3\text{As}_{10}$.

Table 1. Crystal Data and Refinement Parameters

	CaFe_5As_3	$\text{Ca}_3\text{Fe}_8\Box\text{As}_6$	$\text{Ca}_3\text{Fe}_8\text{PtAs}_6$	$\text{Ca}_3\text{Fe}_8\text{PdAs}_6$
structure	$\alpha\text{-CaFe}_5\text{As}_3$	$\alpha\text{-Ca}_3\text{Fe}_8\Box\text{As}_6$	$\alpha\text{-Ca}_3\text{Fe}_8\text{PtAs}_6$	$\beta\text{-Ca}_3\text{Fe}_8\text{PdAs}_6$
composition	CaFe_5As_3	$\text{Ca}_{2.56}\text{Na}_{0.44}\text{Fe}_{7.49}\text{Nb}_{0.51}\text{As}_6$	$\text{Ca}_3\text{Fe}_{7.705}\text{Pt}_{1.295}\text{As}_6$	$\text{Ca}_3\text{Fe}_{6.98}\text{Pd}_{2.02}\text{As}_6$
space group	$P2_1/m$	$P2_1/m$	$P2_1/m$	$Pnma$
Z	2	2	2	4
a (Å)	7.2734(6)	11.331(1)	11.317(1)	26.363(4)
b (Å)	3.8149(3)	3.8078(3)	3.8809(2)	3.8699(5)
c (Å)	9.7577(8)	13.630(1)	13.701(1)	11.330(1)
β (deg)	100.70(1)	106.15(1)	105.96(1)	90
V (Å ³)	266.04(4)	564.84(8)	578.55(5)	1155.9(2)
R1 (obsd/all)	0.033/0.037	0.081/0.134	0.024/0.031	0.037/0.068
wR2 (obsd/all)	0.085/0.094	0.178/0.197	0.066/0.072	0.079/0.081
	$\text{Ca}_3\text{Fe}_8\text{PtAs}_6$	$\text{Ca}_3\text{Fe}_8\text{PdAs}_6$	$\text{Ca}_6\text{Fe}_{11}\text{Pd}_3\text{As}_{10}$	$\text{Ca}_6\text{Fe}_{11}\text{Pt}_3\text{As}_{10}$
structure	$\beta\text{-Ca}_3\text{Fe}_8\text{PtAs}_6$	$\gamma\text{-Ca}_3\text{Fe}_8\text{PdAs}_6$	$\alpha\text{-Ca}_6\text{Fe}_{11}\text{Pd}_3\text{As}_{10}$	$\alpha\text{-Ca}_6\text{Fe}_{11}\text{Pt}_3\text{As}_{10}$
composition	$\text{Ca}_3\text{Fe}_{6.72}\text{Pt}_{2.28}\text{As}_6$	$\text{Ca}_3\text{Fe}_{4.74}\text{Pd}_{4.26}\text{As}_6$	$\text{Ca}_6\text{Fe}_{7.88}\text{Pd}_{6.12}\text{As}_{10}$	$\text{Ca}_6\text{Fe}_{7.62}\text{Pt}_{6.38}\text{As}_{10}$
space group	$Pnma$	$Pnma$	$P2_1/m$	$P2_1/m$
Z	4	4	2	2
a (Å)	26.435(3)	19.856(3)	15.564(3)	15.499(1)
b (Å)	3.9177(10)	3.9461(5)	3.9679(6)	3.9807(2)
c (Å)	11.345(2)	15.343(2)	17.880(3)	17.814(1)
β (deg)	90	90	108.748(5)	109.169(1)
V (Å ³)	1174.9(4)	1202.2(3)	1045.7(3)	1038.1(1)
R1 (obsd/all)	0.051/0.137	0.022/0.066	0.064/0.125	0.036/0.058
wR2 (obsd/all)	0.103/0.113	0.042/0.047	0.142/0.153	0.076/0.081

mixture of the β and γ modifications. An α -type compound has not been identified so far. All samples were characterized by powder X-ray diffraction using a Huber G670 diffractometer with Cu $K\alpha_1$ or Co $K\alpha_1$ radiation. Single crystals were selected from the polycrystalline samples, and X-ray intensity data were measured on a STOE IPDS I or a Bruker D8 QUEST diffractometer. Energy-dispersive X-ray spectroscopy was used to check the compositions. The structure refinements were performed against F^2 using the *Jana2006* program package.¹⁴ Rietveld refinements of the powder diffraction data were performed with the *TOPAS* package¹⁵ by using the structural data obtained by the single-crystal experiments. A typical pattern with a Rietveld fit is exemplarily shown in Figure 1. Up to 10% of impurity phases were detected in the bulk samples, mostly binary arsenides.

RESULTS AND DISCUSSION

During the course of exploration in the field of iron arsenides, five so far unknown crystal structures were identified by single-crystal X-ray structure determination (Table 1). The compounds obey the general composition of $\text{Ca}_{n(n+1)/2}(\text{Fe}_{1-x}\text{M}_x)_{(2+3n)}\text{M}'_{n(n-1)/2}\text{As}_{(n+1)(n+2)/2}$ ($\text{M} = \text{Nb, Pd, Pt}$; $\text{M}' = \Box, \text{Pd, Pt}$) with $n = 1\text{--}3$. They crystallize in monoclinic or orthorhombic crystal systems and feature three-dimensional frameworks of interconnected layers forming parallel channels. Figure 2 depicts the triangular shape of the channels for $n = 1\text{--}3$. With $n > 1$, additional sites occur within the channels, which can be occupied by M' .

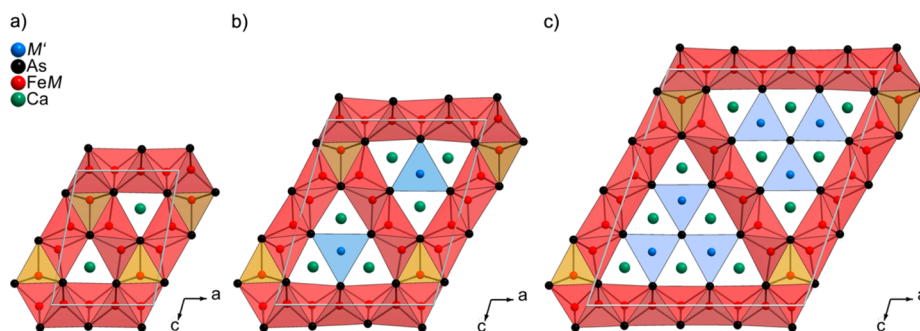


Figure 2. Crystal structures of the monoclinic compounds $\text{Ca}_{n(n+1)/2}(\text{Fe}_{1-x}\text{M}_x)_{(2+3n)}\text{M}'_{n(n-1)/2}\text{As}_{(n+1)(n+2)/2}$ ($M = \text{Pd}, \text{Pt}$; $M' = \square, \text{Pd}, \text{Pt}$) with $n = 1-3$ showing the channel shapes for varying n .

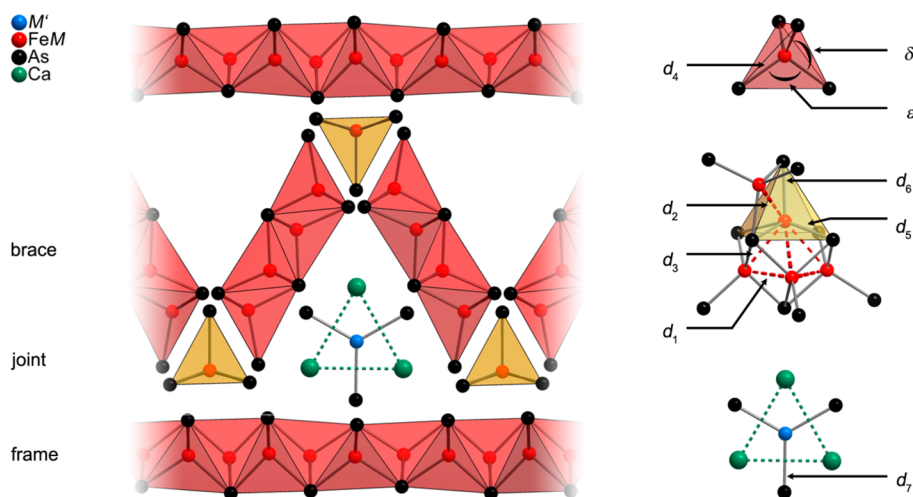


Figure 3. Basic building blocks of the compounds $\text{Ca}_{n(n+1)/2}(\text{Fe}_{1-x}\text{M}_x)_{(2+3n)}\text{M}'_{n(n-1)/2}\text{As}_{(n+1)(n+2)/2}$ (left) and coordination polyhedra and labels for distances and angles (right).

The new structures crystallize in the space groups $P2_1/m$ or $Pnma$, respectively, where they all share a short b axis of about 3.9 Å with atomic sites exclusively on mirror planes at $y = 1/4$ and $3/4$. A three-dimensional framework is formed by covalently bonded and interconnected iron arsenide layers, assembling equilateral triangular channels. Illustrations of the basic building units as well as the designation of labels of distances and angles for a later discussion are depicted in Figure 3. Similar to a scaffold, the framework can be divided into coplanar two-dimensional frames of $\infty_2[\text{Fe}_{2(n+1)}(\text{As}_{4/4})_{2(n-1)}(\text{As}_{4/7})_4]$, diagonal braces $\infty_1[\text{Fe}_{2n}(\text{As}_{4/4})_{2(n-1)}(\text{As}_{3/7})_2(\text{As}_{1/7})_2]$, and joints $\infty_1[\text{Fe}(\text{As}_{2/7})_2\text{As}_{1/7}]$, generally keeping in mind their infinite arrangement along the short b axis. This metaphoric description of the building blocks will be conveniently used for further structure discussion. The channels within the structures are populated with calcium and, depending on the compound composition, as well with arsenic and palladium or platinum in trigonal-planar coordination.

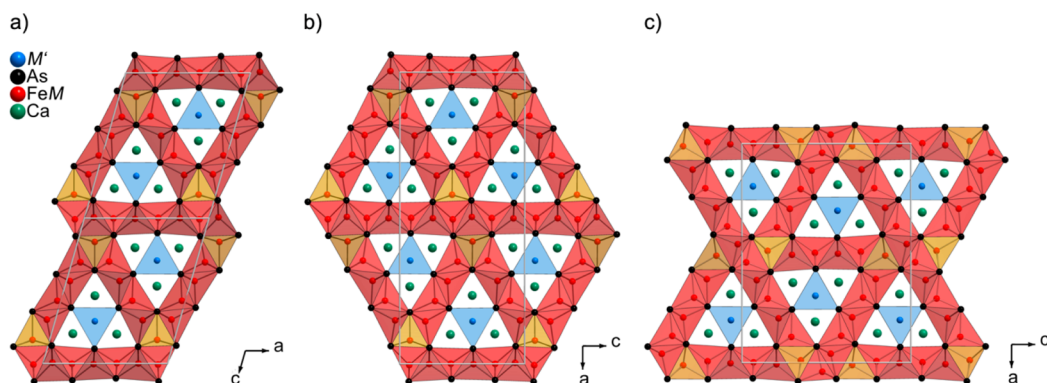
The frames are formed by edge-sharing $\text{FeAs}_{4/4}$ tetrahedral layers corresponding to the *anti*- PbO type. The atomic distances (d_4) and angles (δ and ϵ) are comparable to the values found in the structures of the layered iron arsenides, including in-plane Fe–Fe metal bonding (d_1).⁶ Corresponding features were found for the braces with the mere difference of their restricted extent in the second dimension. A distinctly different situation was found for the joints. There, iron is surrounded by five arsenic atoms in pyramidal coordination. The base plane is formed by a rectangular arrangement of arsenic. Within these

pyramids, the Fe–As bond lengths (d_5 and d_6) are significantly enlarged compared to the tetrahedral layers (d_4). The same situation was found regarding Fe–Fe distances (d_2 and d_3). Thus, the interaction of the braces to the frames is decreased, leading to a certain degree of two-dimensionality conserved in this structures, which can be also seen from the presence of continuous frames, being reminiscent of the layered iron arsenide structures. Nevertheless, the rectangular base plane of the joint pyramids leads to a local distortion within the frames. Therefore, each structure features one very small ϵ angle caused by a frame iron capping the short edge of the pyramid base. Table 2 gives a comparison summary of selected distances and angles for the compounds investigated.

The compounds $\text{Ca}_{n(n+1)/2}(\text{Fe}_{1-x}\text{M}_x)_{(2+3n)}\text{M}'_{n(n-1)/2}\text{As}_{(n+1)(n+2)/2}$ comprise channels of varying size defined by the iron arsenide framework. Thus, depending on its size, each channel is populated with $n(n+1)/2$ calcium atoms, each trigonal-prismatically coordinated by arsenic. These CaAs_6 prisms share faces, giving rise to strands within the channels. Additionally, compounds with $n \geq 2$ feature the possibility to host further metal atoms M' in each center of three edge connected strands, while this particular site is trigonal-planar-coordinated by arsenic. Compounds with a vacancy, palladium, or platinum at this site were found for $n = 2$, and palladium or platinum for a structure with $n = 3$ could be identified so far. Similar planar coordination of palladium and platinum by arsenic was found in CaPtAs and in other compounds.^{16,17} For compounds exceeding $n = 2$, the channel size within the iron

Table 2. Selected Interatomic Distances (Å) and Bond Angles (deg)

	α -CaFe ₅ As ₃	α -Ca ₃ Fe ₈ □As ₆	α -Ca ₃ Fe ₈ PtAs ₆	β -Ca ₃ Fe ₈ PdAs ₆
composition	CaFe ₅ As ₃	Ca _{2.56} Na _{0.44} Fe _{7.49} Nb _{0.51} As ₆	Ca ₃ Fe _{7.71} Pt _{1.29} As ₆	Ca ₃ Fe _{6.98} Pd _{2.02} As ₆
d_1 (Fe–Fe)	2.597(1)–2.763(1)	2.644(1)–2.803(1)	2.602(2)–2.873(1)	2.605(4)–2.850(2)
d_2 (Fe–Fe)	2.982(1)–3.024(1)	2.940(1)–2.958(1)	2.943(1)–2.976(2)	2.948(3)–2.991(3)
d_3 (Fe–Fe)	2.698(1)–2.770(1)	2.780(1)–2.892(1)	2.728(2)–2.959(1)	2.717(4)–2.935(2)
d_4 (Fe–As)	2.383(1)–2.471(1)	2.398(1)–2.462(1)	2.386(1)–2.477(1)	2.383(4)–2.499(2)
d_5 (Fe–As)	2.616(1)–2.624(1)	2.675(1)–2.680(1)	2.657(1)–2.672(1)	2.658(3)–2.684(3)
d_6 (Fe–As)	2.506(1)	2.620(1)	2.570(1)	2.578(3)
ϵ (As–Fe–As)	92.47(3)–106.95(3)	96.43(2)–108.35(1)	92.22(6)–111.22(6)	94.00(12)–111.15(8)
δ (As–Fe–As)	109.42(3)–116.31(3)	109.15(1)–115.27(1)	106.46(1)–115.67(1)	107.52(8)–114.93(14)
d_7 (M–As)			2.479(1)–2.493(1)	2.446(2)–2.460(2)
	β -Ca ₃ Fe ₈ PtAs ₆	γ -Ca ₃ Fe ₈ PdAs ₆	α -Ca ₆ Fe ₁₁ Pd ₃ As ₁₀	α -Ca ₆ Fe ₁₁ Pt ₃ As ₁₀
composition	Ca ₃ Fe _{6.72} Pt _{2.28} As ₆	Ca ₃ Fe _{4.74} Pd _{4.26} As ₆	Ca ₆ Fe _{7.88} Pd _{6.12} As ₁₀	Ca ₆ Fe _{7.62} Pt _{6.38} As ₁₀
d_1 (Fe–Fe)	2.623(2)–2.886(1)	2.683(2)–2.877(1)	2.704(1)–2.883(1)	2.641(1)–2.888(1)
d_2 (Fe–Fe)	2.965(2)–2.998(2)	2.988(1)–3.022(1)	3.023(1)–3.030(1)	2.971(1)–3.003(1)
d_3 (Fe–Fe)	2.696(3)–2.968(2)	2.834(2)–2.959(2)	2.788(1)–2.798(1)	2.721(2)–3.007(1)
d_4 (Fe–As)	2.373(2)–2.551(1)	2.350(2)–2.564(1)	2.362(1)–2.583(1)	2.395(1)–2.578(1)
d_5 (Fe–As)	2.675(2)–2.712(2)	2.743(1)–2.761(1)	2.752(1)–2.765(1)	2.714(1)–2.744(2)
d_6 (Fe–As)	2.558(3)	2.571(2)	2.591(1)	2.553(2)
ϵ (As–Fe–As)	93.63(9)–111.79(6)	99.13(6)–110.97(5)	98.51(1)–112.77(1)	94.90(6)–112.25(5)
δ (As–Fe–As)	105.12(1)–114.85(1)	107.81(5)–113.74(5)	107.58(1)–113.27(1)	107.57(1)–113.82(1)
d_7 (M–As)	2.450(2)–2.459(2)	2.449(1)–2.461(2)	2.442(1)–2.468(1)	2.431(1)–2.448(1)

Figure 4. Different polymorphs of $\text{Ca}_{n(n+1)/2}\text{Fe}_{(2+3n)}\text{M}'_{n(n-1)/2}\text{As}_{(n+1)(n+2)/2}$ with $n = 2$; (a) α -Ca₃Fe₈M'As₆; (b) β -Ca₃Fe₈M'As₆; (c) γ -Ca₃Fe₈M'As₆.

arsenide framework cannot coordinate all calcium atoms anymore. Therefore, additional arsenic is incorporated for $n > 2$, saturating the coordination of calcium. Generally, the iron arsenide frames and braces allow for partial palladium and platinum substitution of the iron sites, whereas hardly any mixing was traceable at the joints. However, adding niobium and sodium to the reaction gives rise to significant Fe/Nb mixing exclusively at the joints and Na/Ca mixing within the channels. Similar results were reported for chromium-doped CaFe₄As₃.¹⁰

The availability of fundamental structural building blocks as frames, braces, and joints allows for a multitude of different structures, facilitating both different arrangements of the channels and different channel sizes with a general composition of $\text{Ca}_{n(n+1)/2}(\text{Fe}_{1-x}\text{M}_x)_{(2+3n)}\text{M}'_{n(n-1)/2}\text{As}_{(n+1)(n+2)/2}$ and $n = 1, 2, 3, \dots$. So far we could identify homologous structures for $n = 1$ –3 as well as three different polymorphs for $n = 2$. Figure 2 illustrates the structures with constant channel arrangement and $n = 1$ –3, while Figure 4 shows the different polymorphs found with constant $n = 2$. The γ -polymorph takes a special position within the presented structure discussion. The frames are intermitted every second channel, therewith losing their infinite extent in one direction.

Considering the case $n = 0$, the general formula of this compound yields Fe₂As. The resulting structure for this type should lack any channels. Indeed, the structure of Fe₂As (Cu₂Sb type) reveals layers of edge-connected FeAs₄ tetrahedra as well as edge-connected FeAs₅ pyramids. Thus, even this long-known binary can be reduced to the basic building units that we described; however, in this special case, braces and channels are absent. Going the other way to the infinite limit $n = \infty$, a hypothetical structure would consist of a mere one “channel” with no iron arsenide frames, braces, and joints presented anymore. CaPtAs might be considered in this context,¹⁸ locally featuring trigonal-planar-coordinated platinum sites as well as edge-connected parallel strands of CaAs₆. Another more distorted representative would be CaPdAs.¹⁹

The view of fundamental building blocks described so far even allows for an easy understanding of the close relationship of our new structures to CaFe₄As reported in 2009.⁹ In this context, the structure of CaFe₄As₃ can be interpreted as a defect polymorph of the compound with $n = 1$ with an ordered vacancy of one iron site. A closer view actually reveals CaFe₄As₃ as the defect γ polytype with $n = 1$. With the frames being discontinuous, the γ -type structures can be understood as two

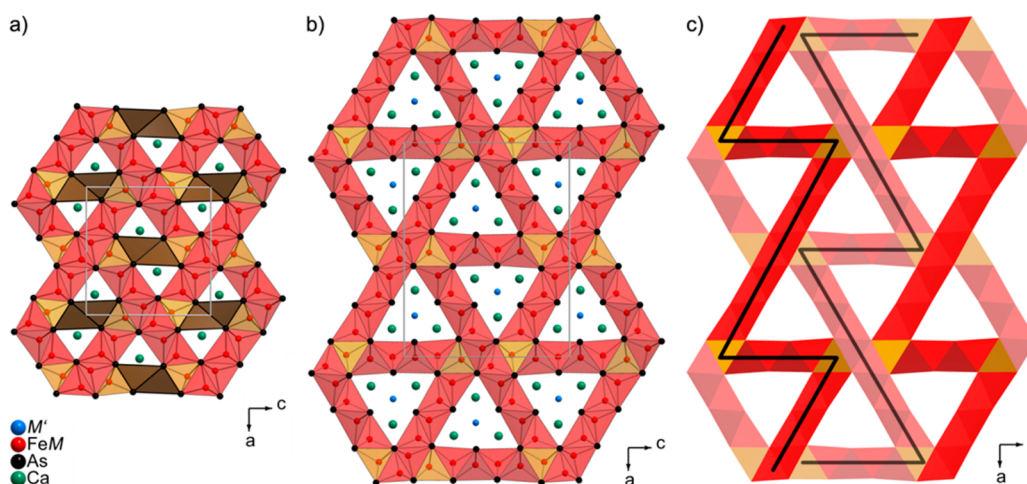


Figure 5. Comparing the structures of CaFe_4As_3 (left) in terms of a defect variant to $\gamma\text{-Ca}_3\text{Fe}_8\text{M}'\text{As}_6$ (middle). Defect sites are highlighted in brown. Sawtooth motif in the γ -type structures (right).

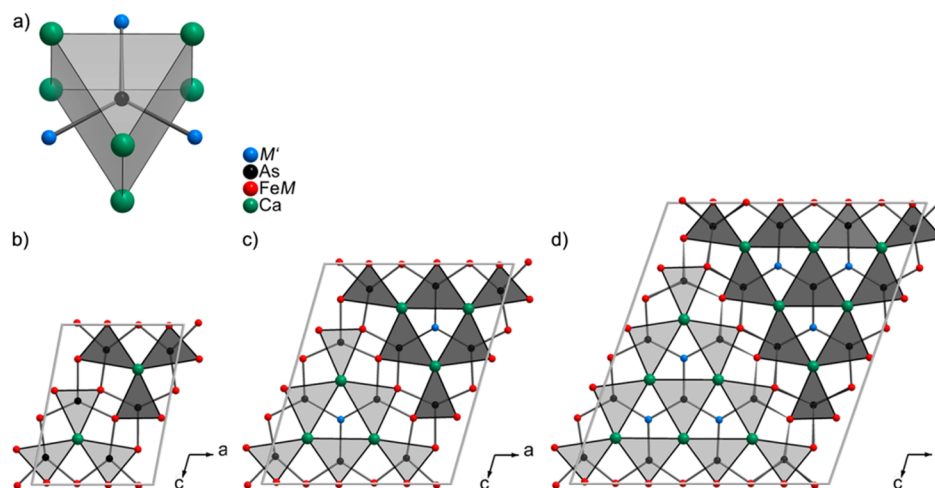


Figure 6. Crystal structures of $\text{Ca}_{n(n+1)/2}(\text{Fe}_{1-x}\text{M}_x)_{(2+3n)}\text{M}'_{n(n-1)/2}\text{As}_{(n+1)(n+2)/2}$ with $n = 1, 2, 3, \dots$, emphasizing the tricapped trigonal-prismatic AsM_9 coordination.

connected sawtooth layers, with each formed by one frame fragment, one brace, and two joints. Figure 5 compares both structures with the defect polyhedra of CaFe_4As_3 highlighted and contains a schematic illustration of the sawtooth-like motif of the γ type.

Although the existence of frameworks built by tetrahedra frames, braces, and pyramidal joints is quite new in the iron arsenide family, it is not exclusively restricted to this class of compounds. Most recently, Khatun et al. reported the structures of $\text{Rb}_4\text{M}_7\text{Pn}_7$ and $\text{Rb}_7\text{M}_{12}\text{Sb}_{12}$ with $M = \text{Mn}, \text{Zn}$, and Cd featuring coplanar zigzag layers of edge-connected MPn_4 tetrahedra including MPn_5 pyramids at every kink.²⁰ In terms of the building block concept that we applied on our structures, these structures may be rationalized as frameworks lacking frames and thus forming zigzag layers of braces and joints.

A different approach of framework transition-metal pnictides and related silicides was given earlier by Jeitschko and co-workers^{21,22} and other authors,^{23,24} reporting, for instance, rare-earth cobalt phosphides featuring structure types very similar to those of our iron arsenides $\text{Ca}_{n(n+1)/2}(\text{Fe}_{1-x}\text{M}_x)_{(2+3n)}\text{M}'_{n(n-1)/2}\text{As}_{(n+1)(n+2)/2}$. They describe these structures in terms of a frequently reappearing relation of metal to pnictide in nature of 2:1,

including also metal-rich binaries like Co_2P . The common building unit is tricapped trigonal-prismatic coordination of the pnictide by metal atoms, whereas the different arrangements of these PnM_9 units yield the large plethora of crystal structures known in this class. The structures of the monoclinic compounds $\text{Ca}_{n(n+1)/2}(\text{Fe}_{1-x}\text{M}_x)_{(2+3n)}\text{M}'_{n(n-1)/2}\text{As}_{(n+1)(n+2)/2}$ with $n = 1-3$ are exemplarily illustrated in Figure 6, emphasizing the tricapped prismatic coordination of the arsenic. In the structures presented in this paper, each arsenic atom is in the center of an AsM_9 unit, with M being all metal atoms present. Within the channels, these units are edge-connected but separated from neighboring channels by FeAs tetrahedra layers. Very similar structures were reported for the compounds HoCo_3P_2 , ScCo_5P_3 , and $\text{Sc}_5\text{Co}_{19}\text{P}_{12}$,²¹ but with different arrangements of the triangular channels and partial incorporation of different channel sizes as well as other building blocks in the same structure.

The iron arsenide framework structures reported in this paper are supposed to feature interesting magnetic and electronic properties. For CaFe_4As_3 , iron(II) was evidenced for tetrahedral coordination and iron(I) in the pyramidal environment.⁹ We have conducted preliminary density functional

theory calculations and found exclusively magnetic ground states for all compounds. Calculated magnetic moments range from ~ 0.3 to $2.0 \mu_B$ at the iron atoms of the frames and braces and up to $\sim 2.5 \mu_B$ at the joints. However, detailed magnetic measurements and neutron diffraction experiments are necessary to prove this. For the time being, it seems reasonable to assume a similar situation of two different iron species for our compounds. Because the compounds $\text{Ca}_{n(n+1)/2}(\text{Fe}_{1-x}\text{M}_x)_{(2+3n)}\text{M}'_{n(n-1)/2}\text{As}_{(n+1)(n+2)/2}$ allow for different distances and arrangements of the iron sites, they present an excellent model system to study the geometry-dependent interplay of a variety of different magnetic centers. Still, no superconductivity was observed yet in any of the compounds described, despite the presence of two-dimensional iron arsenide tetrahedral layers. Nevertheless, these new phases clarify that layered iron arsenide structures are not just restricted to two-dimensional stacking structures but facilitate the formation of complex three-dimensional frameworks.

CONCLUSION

In conclusion, we reported the eight new calcium iron arsenide compounds $\text{Ca}_{n(n+1)/2}(\text{Fe}_{1-x}\text{M}_x)_{(2+3n)}\text{M}'_{n(n-1)/2}\text{As}_{(n+1)(n+2)/2}$ with $n = 1, 2, 3, \dots$, $M = \text{Nb, Pd, Pt}$, and $M' = \square, \text{Pd, Pt}$. The structures reveal three-dimensional frameworks of cross-linked iron arsenide layers with trigonal channels along a short b axis of 3.9 \AA . Thereby the size and arrangement of the channels give rise to the different structures. This relationship was also rationalized by the identification of common structural building blocks and their resemblance to CaFe_4As_3 . The compounds feature coordination of an arsenic typical for compounds with a metal-to-pnictide ratio of 2:1. The identification of these new structures elucidates the structural flexibility of iron arsenide layers toward rearrangements. Unlike CaFe_4As_3 , $\text{Ca}_{n(n+1)/2}(\text{Fe}_{1-x}\text{M}_x)_{(2+3n)}\text{M}'_{n(n-1)/2}\text{As}_{(n+1)(n+2)/2}$ still feature continuous coplanar $\text{FeAs}_{4/4}$ layers and therewith a certain degree of two-dimensionality. Although no superconductivity has been observed in these compounds so far, interesting magnetic and electronic properties are expected.

ASSOCIATED CONTENT

Supporting Information

Crystallographic data in CIF format. This material is available free of charge via the Internet at <http://pubs.acs.org>. Information on the structure determination can be obtained free of charge at Fachinformationszentrum Karlsruhe, 76344 Eggenstein-Leopoldshafen, Germany [fax (+49)7247-808-666; e-mail crysdata@fiz-karlsruhe.de; web site http://www.fiz-karlsruhe.de/request_for_deposited_data.html] upon quoting the CSD numbers 427439 [α -(Ca,Na) $_3(\text{Fe,Nb})_8\text{As}_6$], 427440 (α - $\text{Ca}_3\text{Fe}_8\text{PtAs}_6$), 427441 (α - $\text{Ca}_6\text{Fe}_{11}\text{Pd}_3\text{As}_{10}$), 427442 (α - $\text{Ca}_6\text{Fe}_{11}\text{Pt}_3\text{As}_{10}$), 427443 (α - CaFe_5As_3), 427444 (β - $\text{Ca}_3\text{Fe}_8\text{PdAs}_6$), 427445 (β - $\text{Ca}_3\text{Fe}_8\text{PtAs}_6$), and 427446 (γ - $\text{Ca}_3\text{Fe}_8\text{PdAs}_6$).

AUTHOR INFORMATION

Corresponding Author

*E-mail: dirk.johrendt@cup.uni-muenchen.de.

Notes

The authors declare no competing financial interest.

ACKNOWLEDGMENTS

This work was financially supported by the German Research Foundation (DFG) within the priority program SPP1458. F.N.

was supported by FP7 European project SUPER-IRON (Grant Agreement 283204).

REFERENCES

- (1) Kamihara, Y.; Watanabe, T.; Hirano, M.; Hosono, H. *J. Am. Chem. Soc.* **2008**, *130*, 3296–3297.
- (2) Takahashi, H.; Igawa, K.; Arii, K.; Kamihara, Y.; Hirano, M.; Hosono, H. *Nature* **2008**, *453*, 376–378.
- (3) Ren, Z.-A.; Lu, W.; Yang, J.; Yi, W.; Shen, X.-L.; Li, Z.-C.; Che, G.-C.; Dong, X.-L.; Sun, L.-L.; Zhou, F.; Zhao, Z.-X. *Chin. Phys. Lett.* **2008**, *25*, 2215.
- (4) Johrendt, D. *J. Mater. Chem.* **2011**, *21*, 13726–13736.
- (5) Johrendt, D.; Pöttgen, R. *Angew. Chem., Int. Ed.* **2008**, *47*, 4782.
- (6) Johnston, D. C. *Adv. Phys.* **2010**, *59*, 803–1061.
- (7) Dai, P.; Hu, J.; Dagotto, E. *Nat. Phys.* **2012**, *8*, 709–718.
- (8) Stewart, G. R. *Rev. Mod. Phys.* **2011**, *83*, 1589–1652.
- (9) Todorov, I.; Chung, D. Y.; Malliakas, C. D.; Li, Q. a.; Bakas, T.; Douvalis, A.; Trimarchi, G.; Gray, K.; Mitchell, J. F.; Freeman, A. J.; Kanatzidis, M. G. *J. Am. Chem. Soc.* **2009**, *131*, 5405–5407.
- (10) Todorov, I.; Chung, D. Y.; Claus, H.; Gray, K. E.; Li, Q. A.; Schleuter, J.; Bakas, T.; Douvalis, A. P.; Gutmann, M.; Kanatzidis, M. G. *Chem. Mater.* **2010**, *22*, 4996–5002.
- (11) Nambu, Y.; Zhao, L. L.; Morosan, E.; Kim, K.; Kotliar, G.; Zajdel, P.; Green, M. A.; Rattcliff, W.; Rodriguez-Rivera, J. A.; Broholm, C. *Phys. Rev. Lett.* **2011**, *106*, 037201.
- (12) Walker, D.; Carpenter, M. A.; Hitch, C. M. *Am. Mineral.* **1990**, *75*, 1020–1028.
- (13) Huppertz, H. Z. *Kristallogr.* **2004**, *219*, 330–338.
- (14) Hieke, V.; Dusek, M.; Palatinus, L. *Jana2006: The crystallographic computing system*; Institute of Physics: Praha, Czech Republic, 2006.
- (15) Coelho, A. *TOPAS-Academic*, version 4.1; Coelho Software: Brisbane, Australia, 2007.
- (16) Hieke, C.; Lippmann, J.; Stürzer, T.; Friederichs, G.; Nitsche, F.; Winter, F.; Pöttgen, R.; Johrendt, D. *Philos. Mag.* **2013**, *93*, 3680–3689.
- (17) Löhnert, C.; Stürzer, T.; Tegel, M.; Frankovsky, R.; Friederichs, G.; Johrendt, D. *Angew. Chem., Int. Ed.* **2011**, *50*, 9195–9199.
- (18) Wenski, G.; Mewis, A. Z. *Anorg. Allg. Chem.* **1986**, *543*, 49–62.
- (19) Johrendt, D.; Mewis, A. Z. *Anorg. Allg. Chem.* **1992**, *618*, 30–4.
- (20) Khatun, M.; Stoyko, S. S.; Mar, A. *Inorg. Chem.* **2013**, *52*, 3148–3158.
- (21) Jeitschko, W.; Reinbold, E. J. Z. *Naturforsch.* **1985**, *40b*, 900–905.
- (22) Prots, Y. M.; Jeitschko, W. *Inorg. Chem.* **1998**, *37*, 5431–5438.
- (23) Le Sénéchal, C.; Babizhetskyy, V.; Députier, S.; Pivan, J. Y.; Guérin, R. *J. Solid State Chem.* **1999**, *144*, 277–286.
- (24) Kuz'ma, Y.; Chykhrij, S.; Phosphides In *Handbook on the Physics and Chemistry of Rare Earths*; Gschneidner, K. A., Eyring, L., Eds.; Elsevier Science: Amsterdam, The Netherlands, 1996; Vol. 23, pp 285–433.